

Synthesis, spectroscopic characterization, thermal, and photostability studies of 2-(2'-hydroxy-5'-phenyl)-5-aminobenzotriazole complexes

Moamen S. Refat

Received: 24 November 2009 / Accepted: 19 April 2010 / Published online: 7 May 2010
© Akadémiai Kiadó, Budapest, Hungary 2010

Abstract Three Mn(II), Co(II), and Cu(II) new transition metal complexes of the fluorescence dye: 2-(2'-hydroxy-5'-phenyl)-5-aminobenzotriazole/PBT derived from *o*-aminophenol and *m*-phenylenediamine have been synthesized. The structural interpretations were confirmed from elemental analyses, magnetic susceptibility and molar conductivity, as well as from mass, IR, UV–Vis spectral studies. From the analytical, spectroscopic, and thermal data, the stoichiometry of the mentioned complexes was found to be 1:2 (metal:ligand). The molar conductance data revealed that all the metal chelates are non-electrolytes and the chloride ions exist inside the coordination sphere. The thermal stabilities of these complexes were studied by thermogravimetric (TG/DTG) and the decomposition steps of these three complexes are investigated. The kinetic parameters such as the energy of activation (E^*), pre-exponential factor (A), activation entropy (ΔS^*), activation enthalpy (ΔH^*), and free energy of activation (ΔG^*) have been reported. Photostability of phenyl benzotriazole as fluorescence dye and their metal complexes doped in polymethyl methacrylate/PMMA were exposed to UV–Vis radiation and the change in the absorption spectra was achieved at different times during irradiation period.

Keywords Benzotriazole · Transition metals · Thermal analysis · Thermodynamic parameters

Introduction

Metal–dye complexes play an important role in dyestuff technology [1–12]; chromium, cobalt, copper, nickel, ruthenium, and aluminum derivatives were used most frequently for these purposes [13–17].

The environment pollution has been a major concern of the present industrial societies. The protection from pollution, especially by chemical industries, has put the challenge to chemists and photophysicists in many countries. The determination of heavy and transition metal cations in the environment has been of great interest. Sensors for pollution by metal ions have been of particular actuality [18, 19].

Fluorescent dyes have found application in a number of areas including laser active media [20], potential photo-sensitive biological units [21], fluorescent markers in biology [22], analgesics in medicine [23], light emitting diodes [24], photo-induced electron sensors [25], fluorescence switchers [26], electroluminescent materials [27], liquid crystal displays [28], and ion probes [29].

For instance, azo compounds and their metal complexes and related features are much interested molecules as pigments and optical data storage [30, 31]. By comparison between azo dyes and their metal complexes is more light stable and have a good thermal stability [32, 33].

Photostability of the polymers is one of their most important properties. To solve the problem of polymer stabilization, a number of different stabilizers have successfully been applied [34]. Among them, 2-hydroxyphenylbenzotriazole UV absorbers are of a great interest due to their high photostabilizing efficiency. They are transparent to visible light and are supposed to dissipate the absorbed energy in a harmless manner, i.e., to convert the

M. S. Refat
Faculty of Science, Department of Chemistry,
Suez Canal University, Port Said 42111, Egypt

M. S. Refat (✉)
Faculty of Science, Department of Chemistry, Taif University,
888, Taif, Kingdom Saudi Arabia
e-mail: msrefat@yahoo.com

absorbed photon energy into heat without being chemically affected [35].

The essential target of the present paper is to synthesize, investigate thermal behavior, and detect the coordination power of PBT (Fig. 1) metal chelates, that this ligand contains several donor sites. The coordination behavior of PBT towards transition metal ions was investigated and the data are confirmed with their molar conductance and magnetic moment measurements. The thermal decomposition of the Mn(II), Co(II), and Cu(II) complexes was used to speculate the structures, also the thermal stabilities studies are essential feature in relation to their application as high-photostability materials.

Experimental

Materials

All chemicals used were of the analytical reagent grade. They include *o*-aminophenol and *m*-phenylenediamine (Aldrich), methanol (Fluka), *N,N*-dimethylformamide (DMF), and dimethylsulphoxide (DMSO) (Fluka). $MnCl_2 \cdot 4H_2O$, $CoCl_2 \cdot 6H_2O$, and $CuCl_2 \cdot H_2O$ (Fluka) were used as received. PMMA was purchased from (Aldrich).

Synthesis of PBT and their metal complexes

The 2-(2'-hydroxy-5'-phenyl)-5-aminobenzotriazole (PBT) was synthesized as described in previous procedures [36] with melting point 212–215 °C.

All the Mn(II), Co(II), and Cu(II) of PBT complexes were synthesized by adding a respective metal(II) salts (0.1 mmol; in 10 mL 99% CH_3OH) to a hot solution of PBT (0.2 mmol; in 20 mL 99% CH_3OH). The mixtures were stirred and heated on a hot plate within 60–70 °C for 30 min. Before precipitation process, the Co(II) complex has a deep-brown color and in a solid form the color changed to black. The *m.p* of Co(II)/PBT was >324 °C and the % yield (88%). While, the color of Cu(II) complex in solution manner before precipitation was faint-brown and after that turned to dark-brown precipitate complex with *m.p* = 210 °C with % yield (87%). Concerning Mn(II)/PBT complex, the solution color before precipitation was

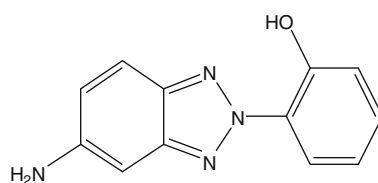


Fig. 1 Structure of synthesized (PBT) fluorescent dye

brownish-yellow and then a brown precipitate complex was formed with *m.p* = 205 °C and % yield (83%). All complexes are isolated in amorphous behavior.

Preparation of dyed polymer matrix: both PMMA grains and dye or its metal complexes were dissolved in chloroform and mixed using a magnetic stirrer. The homogenous mixture was poured into a glass container and allowed to dry.

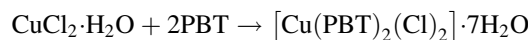
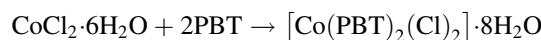
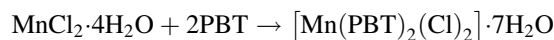
Instrumentals

Carbon, hydrogen, and nitrogen contents were determined using a Perkin-Elmer CHN 2400. The manganese(II), cobalt (II), and copper(II) percentages were estimated gravimetrically by the direct ignition of these complexes at 800 °C for 3 h till constant mass. The residue was then weighed in the forms of metal oxides. IR spectra were recorded on Bruker FT-IR Spectrophotometer ($4000\text{--}400\text{ cm}^{-1}$) in KBr pellets. The UV–Vis spectra were performed in the DMSO solvent with concentration (1.0×10^{-3} M) for the free ligand PBT and their complexes using Jenway 6405 Spectrophotometer with 1 cm quartz cell in the range of 800–200 nm. The solid reflectance spectra were performed on a Shimadzu 3101pc spectrophotometer. The purity was checked from mass spectra at 70 eV using AEIMS 30 mass spectrometer with heating rate of 40 °C/min. Magnetic measurements were carried out on a Sherwood Scientific magnetic balance using Gouy method with $Hg[Co(CNS)_4]$ and $[Ni(en)_3](S_2O_3)$ as a calibrants. Molar conductivities of the freshly prepared solutions with concentration 1.0×10^{-3} mol in DMSO were measured using Jenway 4010 conductivity meter. Thermogravimetric analyses (TG and DTG) were carried out in dynamic nitrogen atmosphere (30 mL/min) with a heating rate of 10 °C/min using a Schimadzu TGA-50H thermal analyzer.

Dye photostability: solar simulator xenon arc lamp “250 w” was used, which had the same spectrum as sun. The degradation of samples was studied by analyzing the UV–Vis absorption spectra. The dye photostability was calculated by dividing the absorbance after exposure to light by that before exposure.

Results and discussion

The chemical reactions mechanisms concerning the interaction between $MCl_2 \cdot nH_2O$ ($M = Mn(\text{II})$, $Co(\text{II})$, and $Cu(\text{II})$) and PBT for the synthesis of PBT metal complexes are as follows:



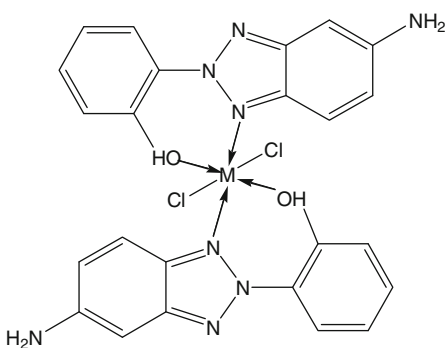


Fig. 2 Structure of PBT complexes (where, $M = \text{Mn}^{\text{II}}$, Co^{II} and Cu^{II})

The molar ratio for all isolated complexes in solid form is 1:2 ($M^{\text{II}}:\text{PBT}$) with the general formula $[\text{M}(\text{PBT})_2(\text{Cl})_2] \cdot n\text{H}_2\text{O}$. The coordination structure of the PBT complexes is given in Fig. 2. The elemental analyses, molar conductance, and magnetic measurements data of the metal chelates of PBT are existed in (Table 1) and in good agreement with those suggested formulas.

Molar conductance measurements

The molar conductivity values ($\Lambda_m/\Omega^{-1}\text{cm}^2 \text{mol}^{-1}$) of the free PBT ligand and their complexes soluble in DMF with 10^{-3} M at 25 °C confirmed that the resultant complexes have non-electrolytic features [37, 38] by comparing the electrolytic nature for each complex with free PBT ligand. The values of the molar conductance data are listed in Table 1.

Infrared spectra and mode of chelation

Interpretation of infrared spectra of free PBT ligand and Mn(II), Co(II), and Cu(II) complexes (Fig. 3) gave an idea about the mode of chelation and follow-up of the effect of coordination of metal ions on the vibration motions of free

ligand. The IR spectra of the free ligand and its metal chelates were carried out within the mid-IR range 4000–400 cm^{-1} (Table 2). The IR spectrum of the free ligand shows a very strong band at 3460 cm^{-1} , which can be attributed to the aryl-OH group [39]. This band is shifted to lower wavenumbers at 3445 and 3405 cm^{-1} in case of Mn(II) and Co(II) complexes, respectively, but this band was absent in case of Cu(II) complex which was assigned to the involvement of OH group in the chelating. The shared aryl-OH group in coordination is confirmed by the hypochromic effect (decrease in intensity) of the $\nu(\text{C}-\text{O})$ stretching band observed at 1250 cm^{-1} in the free ligand and the complexes due to substituents or interactions with the molecular environment [39]. The IR spectrum of the free ligand revealed a very strong-to-strong bands at 1633 and 1598 cm^{-1} due to $\nu(\text{C}=\text{N})$ of the benzotriazole moiety [40–42]. This band is shifted to lower frequencies (30–38 cm^{-1}) in the complexes assigned that it has been affected upon complexation via metal ions. In the 500–400 cm^{-1} region, the spectra of all complexes have a detected bands observed at ~ 550 and 468 cm^{-1} [42], which can be assigned to the $\nu(\text{M}-\text{O})$ and $\nu(\text{M}-\text{N})$ stretching vibrations, respectively. Therefore, the IR spectra indicate that PBT behaves as a bidentate and the coordination sites being ArOH and C=N of the benzotriazole ring.

Electronic absorption spectra of the complexes

The electronic spectra for PBT and its complexes recorded in DMF solvent are given in Table 3. The electronic spectral data of the ligand exhibit more than one band in the UV region. The bands appearing in the range of ~ 230 – 335 nm are attributed to and $\pi-\pi^*$ transition of the ligands. The other bands observed in the region above 340 nm are assigned to $n-\pi^*$ electronic transitions [42, 43]. In the three complexes of PBT, the absorption maxima has a bare close resemblance with the free ligand which indicates that no structural alteration of the ligand has occurred during complexation. However, the values shifted slightly to

Table 1 Elemental analysis, molar conductance and magnetic measurements data of the PBT complexes

Complexes Empirical formula/Mwt	Found/calcd				Molar conductance/ $\Omega^{-1} \text{cm}^2 \text{mol}^{-1}$	μ_{eff}
	C/%	H/%	N/%	M/%		
PBT $\text{C}_{12}\text{H}_{10}\text{N}_4\text{O}/226.23$	63.71/63.66	4.46/4.39	24.76/24.65	—	63.30	—
$[\text{Mn}(\text{PBT})_2(\text{Cl})_2] \cdot 7\text{H}_2\text{O}$ $\text{C}_{24}\text{H}_{34}\text{N}_8\text{O}_9\text{Cl}_2\text{Mn}/704.42$	40.92/40.89	4.86/4.02	15.91/15.87	7.80/7.69	74.70	5.90
$[\text{Co}(\text{PBT})_2(\text{Cl})_2] \cdot 8\text{H}_2\text{O}$ $\text{C}_{24}\text{H}_{36}\text{N}_8\text{O}_{10}\text{Cl}_2\text{Co}/726.43$	39.68/39.57	5.00/4.78	15.43/15.33	8.11/8.05	81.10	5.12
$[\text{Cu}(\text{PBT})_2(\text{Cl})_2] \cdot 7\text{H}_2\text{O}$ $\text{C}_{24}\text{H}_{34}\text{N}_8\text{O}_9\text{Cl}_2\text{Cu}/713.03$	40.43/40.57	4.81/4.78	15.72/15.49	8.91/8.86	65.20	1.10

Fig. 3 IR spectra of: **a** free PBT, **b** Mn^{II}/PBT, **c** Co^{II}/PBT, and **d** Cu^{II}/PBT complexes

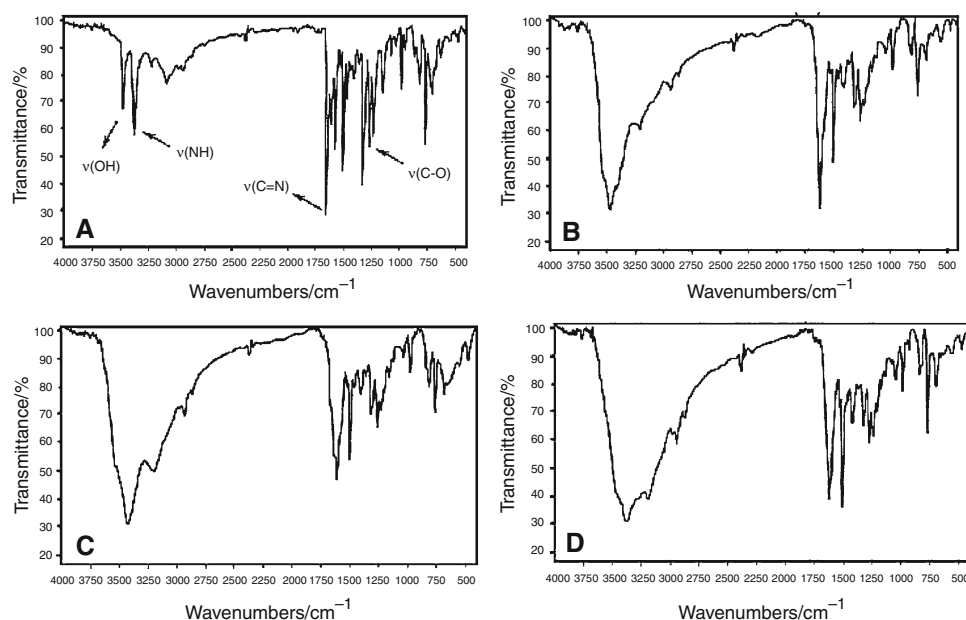


Table 2 Main IR peaks of PBT and its complexes

Compound	ν_{OH}	$\nu_{\text{NH}}; \text{NH}_2$ $\nu_{\text{OH}}; \text{H}_2\text{O}$	$\nu_{\text{CH}}; \text{Ar}$	$\nu_{\text{C}=\text{N}} + \nu_{\text{C}=\text{C}}$ $\delta_{\text{H}_2\text{O}} + \delta_{\text{NH}_2}$	$\nu_{\text{C}-\text{O}}$ $\nu_{\text{C}-\text{N}}$ $\nu_{\text{C}-\text{C}}$	$\nu_{\text{M}-\text{O}}$ $\nu_{\text{M}-\text{N}}$
PBT	3460	3356, 3207	3071, 2968 2925, 2854	1633, 1598, 1561 1519, 1492, 1461 1426, 1403, 1356 1312	1254, 1223 1142, 1066 1032, 975 943, 812	—
Mn ^{II} /PBT	3445	3383, 3191	2924, 2853	1603, 1517, 1490 1452, 1400, 1353 1310	1253, 1222 1192, 1122 1033, 971 808, 753	550, 468
Co ^{II} /PBT	3405	3183	2925, 2853	1599, 1513, 1490 1455, 1400, 1353 1312	1253, 1222 1155, 1033 971, 809 754	551, 469
Cu ^{II} /PBT	—	3354, 3166	2960, 2853	1595, 1515, 1490 1405, 1353, 1311	1256, 1223 1190, 1156 1035, 977 828, 755	552, 468

lower or longer wavelength with absence of two bands at 545 and 575 nm in the free ligand due to the involvement of C=N and OH groups in metal complexation [44].

Magnetic susceptibility and electronic spectra

The diffuse reflectance spectrum of manganese(II) complex display the *d-d* transition bands in the region 625, 615, and 600 nm due to ${}^4\text{T}_{1g} \rightarrow {}^6\text{A}_{1g}$, ${}^4\text{T}_{2g}(\text{G}) \rightarrow {}^6\text{A}_{1g}$ and ${}^4\text{T}_{1g}(\text{D}) \rightarrow {}^6\text{A}_{1g}$, respectively [45, 46]. Manganese(II)

complex exhibits effective magnetic moments of 5.90 BM sp^3d^2 which is present in the region of expected value 5.92–6.00 BM corresponding to five unpaired electrons. The transitions corresponds to the octahedral environment of the Mn(II) complex. The electronic spectrum of Co(II) complex show the *d-d* transition bands in the region, 770, 588, and 468 cm^{-1} . These transitions are probably assigned to the $v_1 = {}^4\text{T}_{1g}(\text{F}) \rightarrow {}^4\text{T}_{2g}(\text{F})$, $v_2 = {}^4\text{T}_{1g}(\text{F}) \rightarrow {}^4\text{A}_{2g}(\text{F})$ and $v_3 = {}^4\text{T}_{1g}(\text{F}) \rightarrow {}^4\text{T}_{2g}(\text{P})$, respectively. Cobalt(II) complex has a magnetic moment of 5.12 BM indicating the presence

Table 3 Electronic spectra of the PBT and its complexes

Compounds	$\lambda_{\text{max}}/\text{nm}$	Assignments
PBT	240, 245, 250, 255, 260, 265 270, 285, 295, 300, 325 340, 345, 390, 395, 545, 575	$\pi-\pi^*$ $n-\pi^*$
Mn ^{II} /PBT	240, 250, 265, 295, 325 340, 355, 390	$\pi-\pi^*$ $n-\pi^*$
Co ^{II} /PBT	235, 240, 245, 260, 265, 300 320, 325, 335 340, 345, 350, 360, 390, 395	$\pi-\pi^*$ $n-\pi^*$
Cu ^{II} /PBT	240, 250, 255, 260, 270, 275 285, 295, 300, 310, 325, 330 340, 345, 350, 355, 360, 390, 395	$\pi-\pi^*$ $n-\pi^*$

of three unpaired electrons and the transitions correspond to the octahedral geometrical structure [45, 46]. The spectrum of Cu(II) complex gives the band centered at 840 nm which may be assigned to ${}^2\text{Eg} \rightarrow {}^2\text{T}_{2g}$ transition in an approximately octahedral environment ($\mu_{\text{eff}} = 1.10$ BM).

Mass spectra

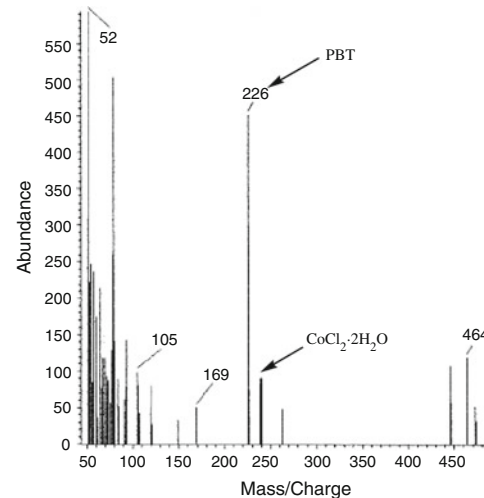
In the mass spectrum of $[\text{Co}(\text{PBT})_2(\text{Cl})_2] \cdot 8\text{H}_2\text{O}$, both peaks at $m/z = 226$ and 238 refer to the molecular ion peak of PBT ligand and $\text{CoCl}_2 \cdot 2\text{H}_2\text{O}$ (Fig. 4). The other fragments assigned to the fragmentation pattern of PBT ligand at 169, 105, and 52.

Thermal analysis and thermodynamic data

Thermal analysis curves (TG/DTG) of the PBT and their Mn(II), Co(II), and Cu(II) transition metal complexes were studied and interpreted in Table 4 and Fig. 5.

The PBT ligand melts at about ~ 212 – 215 °C with simultaneous decomposition. The first mass loss was observed at 261 °C. From the TG curve, it appears that the sample decomposes in only one stage over the temperature range 30 – 800 °C. This step occurs at $(150$ – 300 °C) with a mass loss of (obs. = 98.50%, calc. = 100.00%) due to loss of $\text{C}_{12}\text{H}_{10}\text{N}_4\text{O}$, the difference between the calculated and observed data back to the residual carbon.

The thermal decomposition of Mn(II) complex occurs within five steps. The first degradation step takes place in the range of 30 – 75 °C and it corresponds to the elimination of H_2O molecules with a mass loss of (obs. = 2.10%, calc. = 2.55%). The second step falls in the range of 75 – 140 °C which is assigned to the loss of $2\text{H}_2\text{O}$ molecule with a mass loss (obs. = 4.50%, calc. = 5.11%). Third decomposition step existed within the range 140 – 215 °C and was accompanied by mass loss of (obs. = 4.37%, calc. = 5.11%) which is assigned to loss of $2\text{H}_2\text{O}$. The fourth and final

**Fig. 4** Mass spectrum of $[\text{Co}(\text{PBT})_2(\text{Cl})_2] \cdot 8\text{H}_2\text{O}$ complex

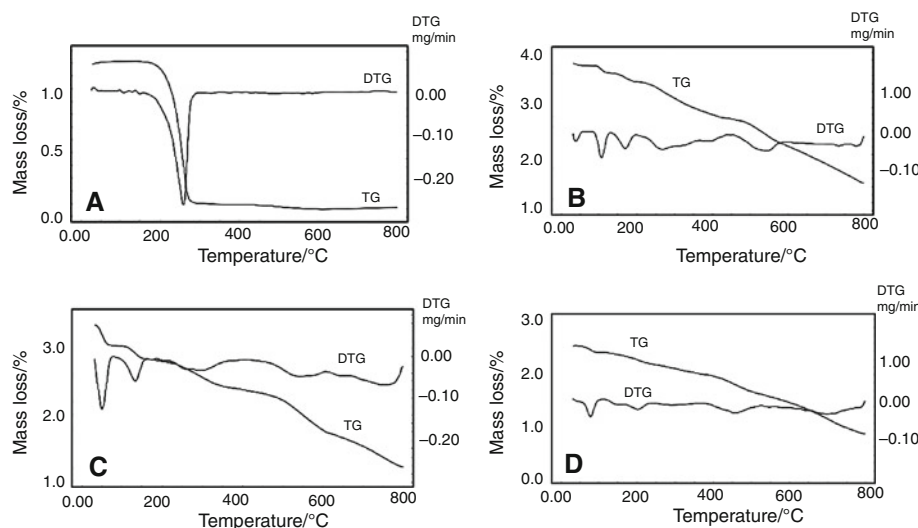
decomposition step exhibited within the range 215 – 800 °C and interpretive accordance the loss of $2\text{H}_2\text{O}$, Cl_2 , and $\text{C}_9\text{H}_{20}\text{N}_8$ organic moiety with mass loss (obs. = 33.14%, calc. = 34.07%). The MnO_2 and contaminated carbon atoms are the final products that remain stable till 800 °C.

The thermal decomposition of cobalt(II) complex occurs completely in five steps. The first step ranged at 30 – 100 °C corresponding to the loss of $4\text{H}_2\text{O}$ molecules representing a mass loss of (obs. = 9.59%, calc. = 9.91%). The second and third steps occurring within 100 – 350 °C range corresponding to the loss of remaining $4\text{H}_2\text{O}$ uncoordinated water molecules and chlorine atoms representing a mass loss of (obs. = 19.93%, calc. = 19.68%). The fourth and fifth steps occur within the temperature range 350 – 800 °C which refer to the decomposition of PBT moiety at $\text{DTG}_{\text{max}} = 538$ and 753 °C, respectively, the mass loss is (obs. = 33.49%, calc. = 34.41%). The CoO and the pollutant carbon atoms are the final products that remain stable till 800 °C.

The thermal degradation of the Cu(II) complex occurs in mainly five degradation stages. The first stage of decomposition occurs at a temperature maximum of 47 °C. The found mass loss associated with this step is (obs. = 5.41%, calc. = 5.05%) and may be attributed to the loss of $2\text{H}_2\text{O}$ molecules. The second and third steps of decomposition occur at temperature maxima of 78 and 202 °C, respectively. The mass loss found at these steps equal to (obs. = 14.18%, calc. = 12.62%) corresponds to the loss of $5\text{H}_2\text{O}$ uncoordinated. The fourth and fifth steps occurring at 250 – 800 °C ($\text{DTG}_{\text{max}} = 455$ and 698) correspond to the loss of chlorine molecule Cl_2 , 2NH_2 , and $\text{C}_{10}\text{H}_{16}\text{N}_6\text{O}$ organic moiety representing a mass loss of (obs. = 47.62%, calc. = 47.54%). The final thermal product obtained at 800 °C is CuO with residual carbon atoms. The final residual products for all PBT complexes

Table 4 Thermal data of the PBT and their Mn^{II}, Co^{II}, and Cu^{II} complexes

Compounds	Steps	Temp. range/°C	DTG peak/°C	TG mass loss/%		Assignments
				Calc.	Found	
PBT	1st	30–800	261	100.00	98.50	C ₁₂ H ₁₀ N ₄ O/ligand moiety
Mn ^{II}	1st	30–75	37	2.55	2.10	H ₂ O
	2nd	75–140	105	5.11	4.50	2H ₂ O
	3rd	140–215	168	5.11	4.37	2H ₂ O
	4th	215–435	266	15.19	16.20	2H ₂ O + Cl ₂
	5th	435–800	540	34.07	33.14	C ₉ H ₂₀ N ₈ MnO ₂ + residual carbon
Co ^{II}	1st	30–100	49	9.91	9.56	4H ₂ O
	2nd	100–165	131	7.43	6.89	3H ₂ O
	3rd	165–350	288	12.25	13.04	H ₂ O + Cl ₂
	4th	350–600	538	20.65	20.55	C ₇ H ₁₀ N ₄
	5th	600–800	753	13.76	12.94	CH ₁₀ N ₄ O CoO + residual carbon
Cu ^{II}	1st	30–50	47	5.05	5.41	2H ₂ O
	2nd	50–100	78	7.57	8.18	3H ₂ O
	3rd	100–250	202	5.05	6.00	2H ₂ O
	4th	250–550	455	14.44	14.86	Cl ₂ + 2NH ₂
	5th	550–800	698	33.10	32.76	C ₁₀ H ₁₆ N ₆ O CuO + residual carbon

Fig. 5 TG/DTG curves of: **a** free PBT, **b** Mn^{II}/PBT, **c** Co^{II}/PBT, and **d** Cu^{II}/PBT complexes

were checked by infrared spectra and confirmed the formation of oxide feature as the end products.

The thermodynamic activation parameters (Table 5) of the first decomposition process of dehydration such as activation entropy (ΔS^*), pre-exponential factor (A), activation enthalpy (ΔH^*), and Gibbs free energy (ΔG^*) were calculated using the Coats and Redfern and Horowitz-Metzger equations [47, 48]. The negative values of entropy (ΔS^*) for all complexes indicated that these are more ordered reactions [49–53]. The high values of the activation energy, E , of the PBT complexes reveal the high

stability of chelation due to their coordinated bond feature and also helpful to predict the bond strength of ligand towards the metal ions. ΔG is positive while ΔS is negative considered as unfavorable or non-spontaneous reactions. The thermodynamic data obtained with the two methods are in harmony with each other. The activation energy of Mn(II) complex is expected to increase in relation with decrease in their radii [49, 50]. The smaller size of the ions permits a closer approach of the ligand. Hence, the E value in of the Mn(II) complex is higher than that for the other Co(II) and Cu(II) complexes. The correlation coefficients

Table 5 Thermodynamic parameters using the Coats–Redfern/CR and Horowitz–Metzger/HM operated for the PBT and their Cu^{II}, Co^{II}, and Mn^{II} complexes

Compound	Stage	Method	Parameter					Correlation coefficient r^2
			$E^*/\text{kJ mol}^{-1}$	A/s^{-1}	$\Delta S^*/\text{J mol}^{-1} \text{K}^{-1}$	$\Delta H^*/\text{kJ mol}^{-1}$	$\Delta G^*/\text{kJ mol}^{-1}$	
PBT	1st	CR	1.26×10^5	4.42×10^{10}	-4.56×10^1	1.22×10^5	1.45×10^5	0.9936
		HM	1.24×10^5	6.21×10^{10}	-4.28×10^1	1.02×10^5	1.42×10^5	0.9999
		Average	1.25×10^5	5.13×10^{10}	-4.42×10^2	1.12×10^5	1.43×10^5	
Mn ^{II}	1st	CR	1.65×10^5	1.46×10^{23}	-1.58×10^2	1.62×10^5	2.03×10^5	0.9889
		HM	1.83×10^5	1.61×10^{24}	-2.17×10^2	1.08×10^5	2.01×10^5	0.9916
		Average	1.74×10^5	8.78×10^{23}	-1.87×10^2	1.35×10^5	2.02×10^5	
Co ^{II}	1st	CR	1.37×10^5	4.19×10^{21}	-1.49×10^2	1.34×10^5	8.67×10^4	0.9988
		HM	1.44×10^5	2.00×10^{22}	-1.81×10^2	1.42×10^5	8.38×10^4	0.9994
		Average	1.40×10^5	1.20×10^{21}	-1.65×10^2	1.38×10^5	8.52×10^5	
Cu ^{II}	1st	CR	9.72×10^4	5.96×10^{12}	-1.63×10^1	1.96×10^5	9.49×10^4	0.9951
		HM	1.04×10^5	9.53×10^{13}	-2.14×10^1	2.81×10^5	9.34×10^4	0.9934
		Average	1.00×10^5	5.06×10^{12}	-1.88×10^2	2.38×10^5	9.41×10^4	

of the Arrhenius plots of the thermal decomposition steps were found to lie in the range from 0.9889 to 0.9999, showing a good fit with linear function.

The photostability

Under the UV lamp, it is clear that $[\text{Mn}(\text{PBT})_2(\text{Cl})_2] \cdot 7\text{H}_2\text{O}$ complex is more green fluorescent than both the other Cu(II) and Co(II) complexes and also the free ligand itself. Concluded that manganese(II) ions enhance the fluorescence properties of PBT rather than cobalt(II) and copper ions.

It is well known that all organic dyes undergo bleaching after prolonged exposure to sunlight. Dyes for fluorescent collectors have to fulfill particularly stringent conditions in this respect. A great many dyes deteriorate within hours or days in bright sunlight and that, on the other hand, solar collectors are expected to have a lifetime of between 10 and 20 years. A reasonable goal for dye lifetime in fluorescent collector is 5 years, because the most expensive part or the system, namely the solar cells, will not degrade and can stay in place, while the collector plates are exchanged at certain intervals. There are some parameters which have an influence on the photostability of dyes [54]: (i) manufacturing parameters such as additives in the plastic materials, method of polymerization, treatment after polymerization, and dye concentration; (ii) operating parameters such as temperature under illumination, periods without illumination, and temperature during these periods, spectrum of incident light and intensity of incident light.

The photochemical degradation of PBT doped in PMMA occurs only in the presence of suitable optical radiation (Xenon arc lamp power), which produces large local increases in temperature and thermal destruction of the dye molecules.

PBT and Mn(II)/PBT doped in PMMA were exposed indoors to UV–Vis radiation and the change in the absorption spectra was achieved at different times during irradiation period as shown in Figs. 6 and 7. After

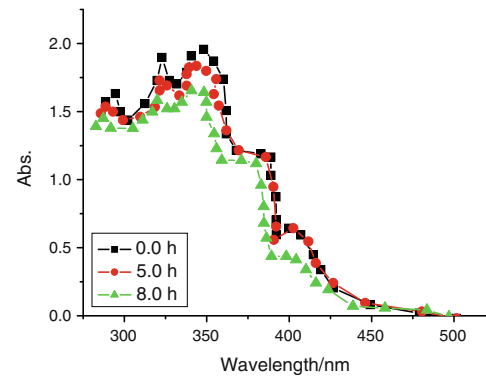


Fig. 6 Photostability of PBT doped in PMMA before and after exposure to UV–Vis light

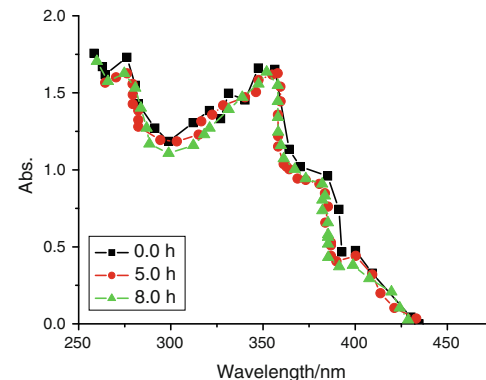


Fig. 7 Photostability of PBT/Mn²⁺ complex doped in PMMA before and after exposure to UV–Vis light

Table 6 Rate constants/k of photodegradation and half life times of doped PBT dye and manganese(II) complex in PMMA

Sample	k/min^{-1}	$t_{1/2}/\text{min}$
PBT/PMMA	385 nm	385 nm
	9.31×10^{-4}	744
PBT/Mn ^{II} complex/PMMA	382 nm	382 nm
	2.18×10^{-4}	3179

complexation, the Mn(II)/PBT enhance the photostability. The increase in photostability is referred to strong chelation between dye with metal ions. The rate constant of photodegradation of dyes was estimated according to the following equation [55, 56]:

$$k = \frac{2.303}{t} \log \frac{A_0}{A}$$

where A_0 and A are the absorptions before and after irradiation for time (t). The k value and half life times are listed in Table 6. It is clear from the degradation data that the complexations modify the photostability of dye.

Acknowledgements The author wishes to express many thanks for the Prof. Ivo Grabchev, Institute of Polymers, Bulgarian Academy of Sciences, Sofia 1113, Bulgaria, for his assistant for supported to a fluorescence dye PBT and the interpretation of photostability measurements.

References

- Gup R, Gizioglu E, Kirkan B. Synthesis and spectroscopic properties of new azo-dyes and azo-metal complexes derived from barbituric acid and aminoquinoline. *Dyes Pigments*. 2007; 73(1):40–6.
- Nejati K, Rezvani Z, Seyedahmadian M. The synthesis, characterization, thermal and optical properties of copper, nickel, and vanadyl complexes derived from azo dyes. *Dyes Pigments*. 2009;83(3):304–11.
- Funaki T, Yanagida M, Onozawa-Komatsuzaki N, Kawanishi Y, Kasuga K, Sugihara H. Ruthenium (II) complexes with π expanded ligand having phenylene–ethynylene moiety as sensitizers for dye-sensitized solar cells. *Sol Energy Mater Sol Cells*. 2009;93(6–7):729–32.
- Funaki T, Yanagida M, Onozawa-Komatsuzaki N, Kasuga K, Kawanishi Y, Sugihara H. A 2-quinoliniccarboxylate-substituted ruthenium(II) complex as a new type of sensitizer for dye-sensitized solar cells. *Inorg Chim Acta*. 2009;362(7):2519–22.
- Anandan S, Madhavan J, Maruthamuthu P, Raghukumar V, Ramakrishnan VT. Synthesis and characterization of naphthyridine and acridinedione ligands coordinated ruthenium (II) complexes and their applications in dye-sensitized solar cells. *Sol Energy Mater Sol Cells*. 2004;81(4):419–28.
- Funaki T, Yanagida M, Onozawa-Komatsuzaki N, Kasuga K, Kawanishi Y, Kurashige M, Sayama K, Sugihara H. Synthesis of a new class of cyclometallated ruthenium(II) complexes and their application in dye-sensitized solar cells. *Inorg Chem Commun*. 2009;12(9):842–5.
- Ning Z, Zhang Q, Wu W, Tian He. Novel iridium complex with carboxyl pyridyl ligand for dye-sensitized solar cells: high fluorescence intensity, high electron injection efficiency. *J Organomet Chem*. 2009;694(17):2705–11.
- Song H-K, Park YH, Han C-H, Jee J-G. Synthesis of ruthenium complex and its application in dye-sensitized solar cells. *J Ind Eng Chem*. 2009;15(1):62–5.
- Polo AS, Itokazu MK, Murakami NY. Metal complex sensitizers in dye-sensitized solar cells. *Coord Chem Rev*. 2004;248(13–14):1343–61.
- Gordon KC, Walsh PJ, McGale EM. Electroluminescence from PVK-based polymer blends with metal complex dyes. *Curr Appl Phys*. 2004;4(2–4):331–4.
- Duprez V, Biancardo M, Krebs FC. Characterisation and application of new carboxylic acid-functionalised ruthenium complexes as dye-sensitisers for solar cells. *Sol Energy Mater Sol Cells*. 2007;91(4):230–7.
- Hara K, Sugihara H, Singh LP, Islam A, Katoh R, Yanagida M, Sayama K, Murata S, Arakawa H. New Ru(II) phenanthroline complex photosensitizers having different number of carboxyl groups for dye-sensitized solar cells. *J Photochem Photobiol A*. 2001;145(1–2):17–22.
- Price R. In: Venkataraman K, editor. The chemistry of synthetic dyes, vol III, chap VII. New York: Academic Press; 1970.
- Baumann H. Ullmanns Encyclopaedie Der Technischen Chemie, vol. 16. Weinheim: Chemie; 1978.
- Ruzicka A, Lycka A, Jambor R, Novak P, Cisarova I, Holcapek M, Erban M, Holecek J. Structure of azo dye organotin (IV) compounds containing a C, N chelating ligand. *Appl Organometal Chem*. 2003;17:168–174.
- Zollinger H. Color chemistry: syntheses, properties and application of organic dyes and pigments. Weinheim: Chemie; 1987.
- Schundehute KH. Methoden der Organischen Chemie (Houben-Weyl), vol. 10/3. Stuttgart: Georg Thieme; 1965.
- de Silva AP, McCaughan B, McKinney BOF, Querol M. Newer optical-based molecular devices from older coordination chemistry. *Dalton Trans*. 2003; 1902–13.
- Rurack K. Flipping the light switch ‘ON’—the design of sensor molecules that show cation-induced fluorescence enhancement with heavy and transition metal ions. *Spectrochim Acta A*. 2001;57:2161–95.
- Martin E, Weigand R, Pardo A. Solvent dependence of the inhibition of intramolecular charge-transfer in N-substituted 1,8-naphthalimide derivatives as dye lasers. *J Lumin*. 1996;68:157–64.
- Tao Z-F, Qian X. Naphthalimide hydroperoxides as photonucleases: substituent effects and structural basis. *Dyes Pigments*. 1999;43:139–45.
- Zheng YM, An Z-X, Zhao X-E, Quan F-S, Zhao H-Y, Zhang Y-R, Liu J, He X-Y, He X-N. Comparison of enhanced green fluorescent protein gene transfected and wild-type porcine neural stem cells. *Res Vet Sci*. 2010;88(1):88–93.
- de Souza MM, Correa R, Cechinel Filho V, Grabchev I, Bojinov V. 4-Nitro-1,8-naphthalimides exhibit antinociceptive properties. *Pharmazie*. 2002;56:430–1.
- Facoetti H, Robin P, Le Barny P, Schott M, Bouche CM, Berdague P. Side-chain electroluminescent polymers. *Synth Met*. 1996;81(2–3):191–5.
- Grabchev I, Chovelon JM, Qian X. A copolymer of 4-N,N-dimethylaminoethylene-N-allyl-1,8-naphthalimide with methylmethacrylate as a selective fluorescent chemosensor in homogeneous systems for metal cations. *J Photochem Photobiol A*. 2003;158(1):37–43.
- Poteau X, Brown A, Brown R, Holmes C, Matthew D. Fluorescence switching in 4-amino-1,8-naphthalimides: “on-off-on” operation controlled by solvent and cations. *Dyes Pigments*. 2000; 47:91–105.

27. Zhu W, Hu M, Yao R, Tian H. A novel family of twisted molecular luminescent materials containing carbazole unit for single-layer organic electroluminescent devices. *J Photochem Photobiol A.* 2003;154:169–77.
28. Grabchev I, Moneva I, Wolarz E, Bauman D. New unsaturated 1,8-naphthal-imide dyes for use in nematic liquid crystals. *Z Naturforsch.* 1996;51:1185–91.
29. Cosnard F, Wintgens V. A new fluoroionophore derived from 4-amino-N-methyl-1,8-naphthalimide. *Tetrahedron Lett.* 1998;39: 2751–4.
30. Zollinger H. Color chemistry syntheses, properties, and applications of organic dyes. Weinheim: VCH; 1987.
31. Nishihara H. Multi-mode molecular switching properties and functions of azo-conjugated metal complexes. *Bull Chem Soc Jpn.* 2004;77(3):407–28.
32. Geng Y, Gu D, Gan F. Application of novel azo metal thin film in optical recording. *Opt Mater.* 2004;27(2):193–7.
33. Bin W, Yi-Qun W, Dong-Hong G, Fu-Xi G. Optical parameters and absorption of azo dye and its metal-substituted compound thin films. *Chin Phys Lett.* 2003;20(9):1596–9.
34. Ranby B, Rabek J. Photodegradation, photooxidation and photostabilization of polymers. London: Wiley; 1975.
35. Crawford JC. 2(2-hydroxyphenyl)2H-benzotriazole ultraviolet stabilizers. *Prog Polym Sci.* 1999;24(1):7–43.
36. Bojinov V, Grabchev I. Synthesis and properties of new adducts of 2,2,6,6-tetramethylpiperidine and 2-hydroxyphenylbezotriazole as polymer photostabilizers. *J Photochem Photobiol A.* 2002;150: 223–31.
37. Refat MS. Complexes of uranyl(II), vanadyl(II) and zirconyl(II) with orotic acid “vitamin B13”: synthesis, spectroscopic, thermal studies and antibacterial activity. *J Mol Struct.* 2007;842:24–37.
38. Refat MS. Synthesis and characterization of norfloxacin-transition metal complexes (group 11, IB): spectroscopic, thermal, kinetic measurements and biological activity. *Spectrochim Acta A.* 2007;68:1393–405.
39. Nakanishi K, Solomon PH. Infrared absorption spectroscopy. 2nd ed. USA: Holden-Day, Inc; 1977.
40. Pandey G, Narang KK. Synthesis, characterization, spectral studies, and antifungal activity of Mn(II), Fe(II), Co(II), Ni(II), Cu(II), and Zn(II) complexes with monosodium 4-(2-pyridylazo)resorcinol. *Synth React Inorg Met Org Chem.* 2005;34:291–311.
41. Roy R, Chattopadhyay P, Sinha C, Chattopadhyay S. Synthesis, spectral and electrochemical studies of arylazopyridine complexes of palladium(ii) with dioxolenes. *Polyhedron.* 1996;15:3361–9.
42. Karipcin F, Kabalcilar E. Spectroscopic and thermal studies on solid complexes of 4-(2-pyridylazo)resorcinol with some transition metals. *Acta Chim Slov.* 2007;54:242–7.
43. Naskar S, Biswas S, Mishra D, Adhikary B, Falvello LR, Soler T, Schwalbe CH, Chattopadhyay SK. Studies on the relative stabilities of Mn(II) and Mn(III) in complexes with N_4O_2 donor environments: crystal structures of [Mn(pybhz)2] and [Mn(Ophsal)(imzH)2] ClO₄ (pybhz = *N*-(benzoyl)-*N'*-(picolinylidene) hydrazine, Ophsal = *N,N*-*o*-phenylenebis(salicylideneimine), imzH = imidazole). *Inorg Chim Acta.* 2004;357:4257–64.
44. Krishnankutty K, Ummathur MB, Sayudevi P. Metal complexes of Schiff bases derived from dicinnamoylmethane and aromatic amines. *J Agent Chem Soc.* 2008;96(1–2):13–21.
45. Earnshaw A. Introduction to magnetochemistry. New York: Academic Press Inc.; 1968.
46. Lever ABP. Inorganic electronic spectroscopy. 1st ed. Amsterdam: Elsevier; 1968.
47. Coats W, Redfern JP. Kinetic parameters from thermogravimetric data [12]. *Nature.* 1964;201:68–9.
48. Horowitz HW, Metzger G. A new analysis of thermogravimetric traces. *Anal Chem.* 1963;35:1464–8.
49. Abd El-Wahed MG, Refat MS, El-Megharbel SM. Synthesis, spectroscopic and thermal characterization of some transition metal complexes of folic acid. *Spectrochim Acta A.* 2008;70(4): 916–22.
50. Abd El-Wahed MG, Refat MS, El-Megharbel SM. Spectroscopic, thermal and biological studies of the coordination compounds of sulfasalazine drug: Mn(II), Hg(II), Cr(III), ZrO(II), VO(II) and Y(III) transition metal complexes. *Chem Pharm Bull.* 2008;56(11): 1585–91.
51. Omar MM. Spectral, thermal and biological activity studies on ruthenium(II) complexes with some pyridylamines. *J Therm Anal Calorim.* 2009;96:607–15.
52. Rotaru A, Gos AM, Rotaru P. Computational thermal and kinetic analysis. Software for non-isothermal kinetics by standard procedure. *J Therm Anal Calorim.* 2008;94:367–71.
53. Verma RK, Verma L, Bhushan A, Verma BP. Thermal decomposition of complexes of cadmium(II) and mercury(II) with tri-phenylphosphanes. *J Therm Anal Calorim.* 2007;90:725–9.
54. Zastrow A. Physics and applications of fluorescent concentrators: a review (Proceedings Paper). Proceedings of SPIE, vol 2255. 1994.
55. Grabchev I, Bojinov V. Synthesis and characterisation of fluorescent polyacrylonitrile copolymers with 1,8-naphthalimide side chains. *Polym Degrad Stab.* 2000;70:147–53.
56. Grabchev I, Bojinov V. Synthesis and characterisation of fluorescent polyacrylonitrile copolymers with 1,8-naphthalimide side chains. *Polym Degrad Stab.* 2001;74:543–50.